IEEE Access
Multidisciplinary | Rapid Review | Open Access Journal

A Robust Technique for Detecting Glaucoma from Fundus

Oluwatobi J. Afolabi[1], Fulufhelo V. Nelwamondo[2], Gugulethu P. Mabuza-Hocket[3] and Babu S. Paul[4]

[1]Department of Electrical/Engineering Science, University of Johannesburg, Johannesburg, South Africa
[2]Nextgen Enterprises & Institutions, Council for Scientific and Industrial Research, Pretoria, South Africa
[3]Defence & Security, Council for Scientific and Industrial Research, Pretoria, South Africa
[4]Institute for intelligent systems, University of Johannesburg, Johannesburg, South Africa

Corresponding author: Oluwatobi J. Afolabi (e-mail: Joshua.aoj@gmail.com).

ABSTRACT Glaucoma has been credited to be the foremost cause of preventable loss of sight in the world second only to cataract. Its effect on the eye is usually irreversible and can only be prevented by early detection. In this paper, we developed a glaucoma detection technique. This technique includes a modified U-net model and an extreme gradient boost (XGB) algorithm. The modified U-net model was utilized to segment both the optic cup and the optic disc from the fundus images. The extreme gradient boost algorithm was utilized to analyze extracted features from segmented optic cups and discs and hence detect glaucoma. The modified U-net model was both trained and tested on the DRIONS, DRISHTI-GS, RIM-ONE-V2 and the RIM-ONE-V3 databases. When tested for optic disc segmentation on the four databases, the model achieved the following average dice-scores: 0.96 on RIM-ONE-V3, 0.97 on RIM-ONE-V2, 0.96 on DRIONS, and 0.97 on DRISHTI-GS. The XGB algorithm achieved an accuracy of 88 % and an AUC-ROC of 92.9 % in detecting glaucoma from the segmented optic disc and optic cup. The proposed glaucoma detection technique achieves a state-of-the-art accuracy and useful for observing structural changes in optic cup and optic disc. The advantage of the proposed modified U-net model is that it has much fewer parameters to be trained when compared to the original U-net model and hence faster training time and cheaper training cost.

INDEX TERMS: Fundus image, Glaucoma, Segmentation, U-net

I. INTRODUCTION

Glaucoma is an eye ailment characterized by a growing deterioration of the optic nerve head as well as ganglion cells in the retina [1] [2]. It is a foremost source of preventable loss of sight with no clear symptom at its preliminary stages. About 50% of its victims are not usually aware of its presence [3] [4] [5]. Glaucoma develops as a result of an obstruction to the flow of the aqueous humour in the eye canal. The obstruction results to a continuous rise in the eye pressure and consequently increasing the size of the optic cup as seen in Fig.1. The enlarged optic cup causes a continuous loss of fibres located at the optic nerve and this is perceived as a gradual loss of vision in its victims. In the preliminary stage of the disease, victims have no symptom or sign but as the disease advances, victims notice a narrowing of the visual field beginning from the peripheral [2] [6] [7]. The damaging action of the disease cannot be reversed and if left unchecked may lead to a permanent loss of sight [8]. Therefore, a procedure that allows for speedy detection of the disease is of significant importance.

The diagnosis of glaucoma is typically implemented by assessing variation in the structure of the optic nerve head [9, 10]. One of the methods that has been utilized to identify the presence of glaucoma is the optic Cup-to-Disc Ratio (CDR). The CDR is the ratio of the longitudinal diameter of the optic cup to the longitudinal diameter of the optic disc [11]. The CDR method depends on the accurate segmentation of the optic disc as well as the optic cup. Several techniques have been utilized to segment the optic disc and the optic cup. The mostly utilized technique involves (i) the pre-processing of fundus image (ii) determining the regions in the fundus image which are of interest (iii) localizing the optic disc (OD) and finally localizing the optic cup (OC). This technique has been utilized in many studies [12-17] with little variation in its implementation. However, the technique is computationally intensive especially when it is tested on large batches of fundus images. This is because the technique must be applied to each of the fundus images individually. Moreover, the accuracy of the technique is substantially influenced by the differing pixel intensities of the fundus images from one database to the other. Therefore, the above-explained technique is not robust to noise and presence of pathologies in the fundus images.

The rest of this paper is arranged as follows: related work is discussed in section 2, the proposed experimental approach is discussed in section 3, section 4 presents the achieved

experimental results, section 5 presents the discussion and analysis of the achieved results, section 6 discusses the limitation of the study, section 7 presents the conclusion and the last section presents the future work.

II. RELATED WORK

Modern advances in object recognition and image processing has brought about the application of deep learning models and systematic algorithms for image segmentation. Maninis *et al*. [20] proposed a method that utilized transfer learning technique to train convolutional neural networks (CNN) [18] which was built on VGG-16 architecture [19]. The proposed method was utilized to segment the OD and OC from fundus images. Maninis *et al*. recorded a dice score of 0.96. The dice score as well as Intersection-over-Union (IoU) score are metrics utilized to measure the goodness of a segmentation process. A good segmentation process will have high dice and IoU scores. Zilly *et al.* [16] utilized a technique that included the use of boosted CNN, filtered entropy [21], normalized contrast and standardized patches to segment the optic cups from fundus images. The AdaBoost algorithm [22] was utilized for the boosting operation. The proposed method was assessed using the DRISHTI-GS database [23] [24] and the RIM-ONE database [25]. The method achieved a dice and IoU score of 0.85 and 0.87 respectively. Improving on what was done by Zilly *et al*., Buhmann *et al.* [26] proposed a new method which does not require the cropping of the disc location before segmenting the optic cup. This method includes a process that picks points holding salient information on the fundus image by using entropy sampling. This method does well by eliminating the computational complexity involved in the method proposed by Zilly *et al.* The method achieved higher dice-score than Zilly *et al*. [16] but a lower IoU score.

After a successful segmentation process, the CDR is usually utilized to detect glaucoma. The CDR method of detecting glaucoma was employed by Patel *et al.* [27].

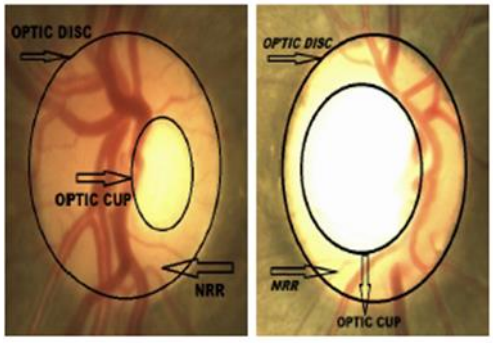

(a) (b)

FIGURE 1 (a) A fundus image with a non-glaucomatous optic cup. (b) A fundus image with an enlarged glaucomatous cup.

In their work, a CDR threshold value of 0.5 was utilized to classify fundus image to either the glaucomatous or the non-glaucomatous class i.e fundus images with CDR values less than or equal to 0.5 were considered non-glaucomatous and CDR values higher than 0.5 were considered glaucomatous.

In a study done by Virk *et al.* [29], 50 fundus images were classified into either the glaucoma or non-glaucoma class. Virk *et al.* concluded that fundus images with CDR values between 0.3 and 0.5 should be classified non-glaucomatous while those of above 0.5 should be classified as glaucomatous. Virk *et al.* recorded an accuracy of 80% when these threshold values were utilized to detect glaucoma. In another study done by Mohamed *et al*. [30], fundus images from the RIM-ONE database were tested for glaucoma. The testing algorithm included the CDR method and a CDR threshold of 0.6 was utilized. Mohamed *et al*. concluded that CDR values for non-glaucomatous fundus images fall between 0.4 and 0.6 and those of glaucomatous fundus images are higher than 0.6. After segmenting the optic cups and optic discs from fundus images, Mvoulana *et al.* [31] employed the CDR method to detect glaucoma. In their study, a CDR threshold value of 0.63 was employed to classify fundus images to either glaucomatous or non-glaucomatous. Fundus images with CDR values greater than 0.63 were classified glaucomatous. Murthi *et al.* [32] used the least square fitting algorithm to segment the optic cups and the optic discs from the fundus images. After the segmentation process, the ellipse fitting algorithm was utilized to smoothen the boundaries of the disc and cup. Murthi *et al.* further utilized the CDR method to detect glaucoma. A CDR threshold value of 0.65 was utilized. For example, fundus images which have CDR values of 0.68 were considered glaucomatous. Khan *et al.* [33] separated the optic cups and optic discs utilizing the mean threshold morphological technique. Together with several attributes, a CDR threshold value of 0.5 was used to recognize glaucomatous fundus images. Lotankar *et al.* [35] suggested a technique for detecting glaucoma by extracting several attributes from the optic nerve head. Attributes extracted from the optic nerve head included the rim to disc area ratio, the cup to disc area ratio and the cup to disc ratio. Lotankar *et al.* proposed that CDR values for non- glaucomatous fundus images range from 0.2 to 0.4 and 0.5 to 1 for glaucomatous fundus images. Roslin *et al*. [34] segmented the blood vessels in the optic discs by using an edge detection algorithm which was based on the Prewitt operators. In their method, the CDR of each fundus image was measured. The authors proposed that the phases of glaucoma development can be studied from the CDR values of the fundus images. In order to classify fundus images into glaucomatous or non-glaucomatous, a CDR threshold value of 0.3 was utilized. Fundus images that have CDR threshold values of 0.3 or less were labelled non-glaucomatous and fundus images which have CDR threshold values that are higher than 0.3 were labelled glaucomatous.

From the above discussion, it has been shown that different CDR threshold values have been utilized to detect glaucoma.

Also, the CDR threshold values utilized depended largely on the dataset and much more on the judgement of the authors.

The following are the contributions of this paper. (1) A proposed segmentation model that is anchored on a modified U-net architecture. The modified U-net architecture has significantly fewer parameters than the traditional U-net. (2) A segmentation algorithm that yields a high dice-score for OC and OD segmentation. (3) A glaucoma classification algorithm based on the extreme gradient boost (XGB). An algorithm that eliminates the challenges of varying CDR threshold values when using the CDR method for glaucoma detection.

III. PROPOSED EXPERIMENTAL APPROACH

A. IMAGE DATABASE

The experiment performed in this work made use of four publicly available databases. The databases consist of fundus images and their corresponding segmented optic discs and optic cups for model training and testing respectively. The databases are RIM-ONE v2 [25], RIM-ONE v3 [25], DRIONS [36] and DRISHTI-GS [23, 24].

The RIM-ONE database was exclusively developed to focus on optic nerve head segmentation. The fundus images are of high resolution captured using a Nidek AFC-210 fundus camera. The camera has a body of Canon EOS 5D mark II and has a resolution of 21.1 megapixels. The version 2 of the database (RIM-ONE v2) has 455 images including 318 training images and 137 testing images. However, the version has only segmented optic discs ground truth and no optic cups ground truth. The version 3 (RIM-ONE v3) has 159 images including 127 images for model training and 32 images for testing. The ground-truth images were provided by two ophthalmologists.

The DRIONS database consists of 110 fundus images. The fundus images belong to subjects with glaucoma and eye hypertension diseases. The images were selected from an eye database that belongs to the Ophthalmology Service at Miguel Servet Hospital, Spain.

The DRISHTI-GS database includes 50 fundus images. The images are high- resolution with a dimension of 2896 x 1944. The ground-truth images were provided by 4 experts. The database consists of both the cup and disc ground-truths.

B. NETWORK ARCHITECTURE

The technique adopted in this research is a combination of two phases. The first phase consists of a segmentation process and the second phase is a detection process. The segmentation process is built on a modified U-net model while the detection phase is built using an extreme gradient boost (XGB) classifier.

The original U-Net model [37] is a convolutional network that has been widely utilized for biomedical image segmentation. It was conceived as an improvement over the Fully Convolutional Network [38]. The network has two layers: the down-sampling encoding layer and the up-sampling decoding layer. The encoding layer is made of two batches of 3 x 3 convolutional layers connected to an activation layer. The activation layer (rectified linear unit ReLU) is followed by a 2 x 2 max-pooling layer. This configuration is then repeated in successions. The decoding layer concatenates the up-sampled feature maps with the output of the encoding layer. The up-sampling was done using 2x2 convolutional layers. The architecture has been widely utilized and has proven to be efficient for segmentation processes [39-42].

In this work, the segmentation process was done using a modified U-Net model as seen in Fig.2. When compared to the original U-Net model, the proposed model has more convolutional layers and has the same size of filters (i.e 3x3) in both the downsampling encoding layer and the upsampling decoding layer. The output layer of the proposed model has a filter size of 1x1. The architecture of the proposed model has significantly fewer parameters than the original U-Net. The original U-net model has about $3.1x10^7$ parameters while our model has $7.8x10^5$ parameters. Our trial showed that models which have huge training parameters over-fit quickly on the data and consequently generalizes poorly on segmentation tasks. We also employed Ioffe and Szeged's [43] batch-normalization on all layers of the model. This brings the mean activation of each layer of the model close to zero. Furthermore, instead of using the rectified linear unit (ReLU) activation, we utilized the leaky rectified linear unit (Leaky ReLU) [44] as seen in equation 1.

$$f(x) = 0.018(x)\ for\ x < 0,$$
$$f(x) = x\ for\ x \geq 0 \quad (1)$$

The Leaky ReLU activation was utilized because it does not saturate quickly and helps the model to converge faster. The output of the proposed model was connected to a 'tanh' activation layer.

The detection process includes a XGB classifier trained with extracted features from the segmented discs and cups. The extracted features were normalized before feeding them into the classifier.

B. SYSTEM WORKING PROCEDURE

The proposed system pipeline is shown in Fig.3. In pursuance of an accurate OC segmentation, the fundus images are cropped based on the location of the OD (the OD location was acquired from the OD segmentation process). This is done in order to accentuate the boundary of the OC. The cropped fundus images are scaled down using spline interpolation of the binomial order and resized to 256 x 256 pixels. The resizing is necessary to enhance the training speed and also allow for more images per batch while training. Prior to passing the re-sized fundus images into the modified U-net model, the contrast of the images is further refined by

stretching out the most frequent intensity values in the images. This process enhances the training of the model and allows it to learn better. The scikit-image histogram-equalization is utilized for this process.

The OD segmentation process is similar to that of the OC except that there is no cropping of the fundus image (as shown by the dotted red jumper arrow in Fig.3). The proposed segmentation process is further described by the following algorithm.

1. Cropping of the fundus images based on the location of the OD. This procedure is needed only for the OC segmentation and not needed for the OD segmentation
2. Applying spline interpolation to the RGB fundus images using the binomial order and nearest mode of filling.
3. Resizing the images to a 256 x 256 pixels.
4. Applying histogram equalization to the images
5. Rescaling of images. All values of images are set to be between 1 and 0.
6. Training the proposed model with the scaled images.

The outputs of the segmentation process (i.e. segmented optic cups and discs) are then post-processed to detect glaucoma. The post-processing steps are described as:

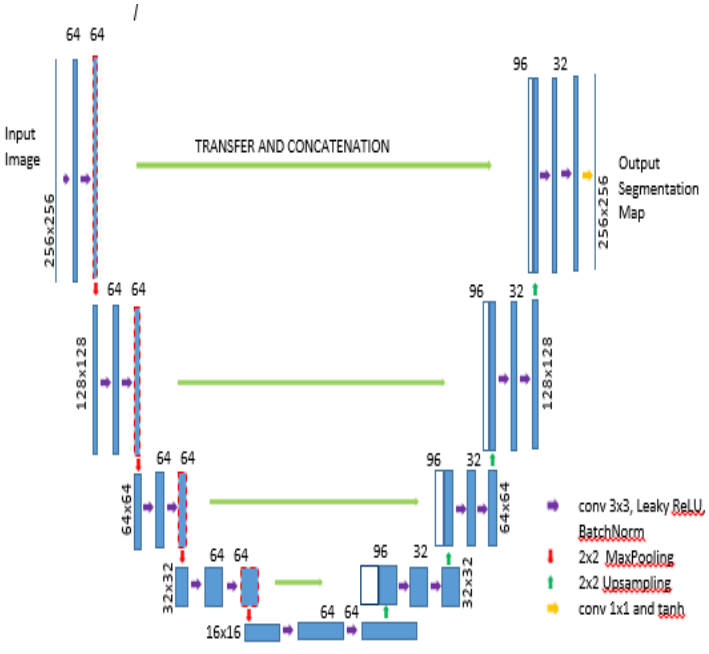

FIGURE 2. The architecture of the proposed model

Step 1: The segmented optic cups and optic discs are masked at 90º. These are the vertical cup and disc features.

Step 2: The maximum values of the non-zero cup and disc features are extracted.

Step 3: The vertical CDR values are acquired by dividing the vertical optic cup length by the vertical optic disc length as shown in equation 2

$$CDR = (Vertical\ cup\ length)\ /\ (vertical\ disc\ length) \quad (2)$$

Step 4: Further extraction of optic cup and disc features from the segmented cups and discs. The extracted features consist of the vertical separation between the cup and disc estimated at 36º spans. This is done to catch the expansion in cup size and the minuscule loss of optic nerves along the optic cup fringe. A total of ten (10) vertical separations (labelled T0-T9) is acquired. This is displayed in Fig.4

Step 5: The vertical cup and its disc length, the horizontal cup and its disc length as well as the diagonal cup and its disc length are acquired and utilized to train a XGB classifier. The vertical, horizontal and diagonal lengths are estimated as shown in Fig. 5 (a) and 5 (b) respectively.

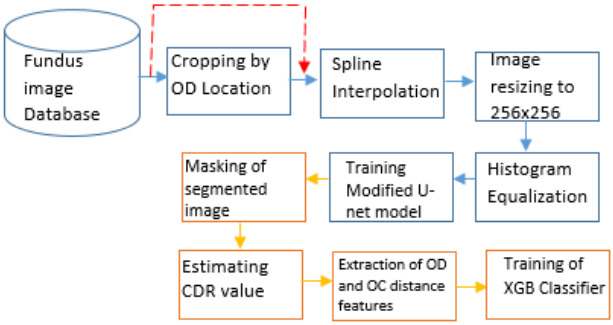

FIGURE 3. CDR value estimation and training of XGB classifier

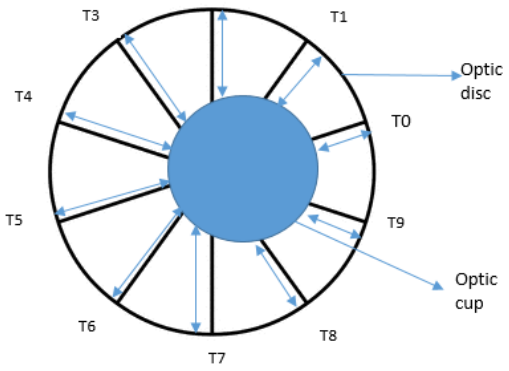

FIGURE 4. Distance between the optic cup and the optic disc evaluated along the optic cup's peripheral

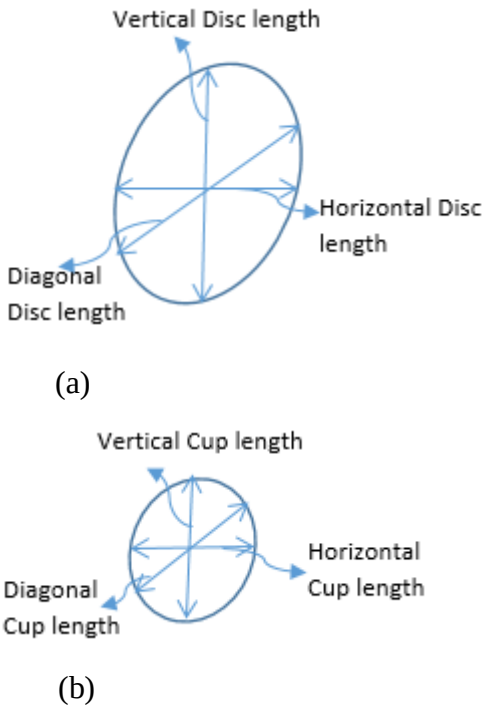

FIGURE 5 (a) The horizontal, diagonal and vertical opti disc lengths. (b) The horizontal, diagonal and vertical optic cup lengths

C. MODEL TRAINING.

The modified U-net model was trained with the four databases discussed in section 2.1. The model was compiled using the Stochastic Gradient Optimizer (SGD) with a learning rate of $1e^{-2}$ for the optic disc segmentation and $1e^{-3}$ for the optic cup segmentation. The Nesterov was set to be true and momentum was set to be 0.95. The loss function utilized in (4) has the same value as the dice-score.

$$f(X,Y) = \frac{2\sum_{i,j}^{h,w} x_{i,j}y_{i,j}}{\sum_{i,j}^{h,w} x_{i,j}^2 + \sum_{i,j}^{h,w} y_{i,j}^2} \quad (3)$$

$$C(X,Y) = -logf(X,Y) \quad (4)$$

where the likelihood that the pixels predicted for the foreground is $X = (x_{i,j})$ and the given output is $Y = (y_{i,j})$, and h, w are the height and width respectively.

A comparative metric to dice-score is the IoU score. The IoU (6) is a metric utilized in many segmentation tasks to quantify the overlay that exists between the ground truth and the output of a model. As seen in (6), it quantifies the pixels present in both the ground truth and the model's output and divides the shared pixel by all the pixels in the ground truth and the model's output. Dice-score (5) is fundamentally the same as IoU, except that it awards more score to each correct pixel in the model's output by increasing the pixels shared by the ground truth and model's output by a factor of 2.

$$D(X,Y) = \frac{2|X \cap Y|}{|X|+|Y|} \quad (5)$$

$$I(X,Y) = \frac{|X \cap Y|}{|X \cup Y|} \quad (6)$$

The model is trained over 65 epochs for both optic cup and optic disc segmentation. The model is trained using Kaggle's 2 CPU cores, 14 GB RAM, 1 NVIDIA Tesla K80 GPU. A batch size of 8 and an image size of 256 by 256 is utilized.

IV. RESULTS

This section evaluates the performance of the proposed segmentation model as well as the trained XGB classifier. Table 1 to Table 4 shows the average results of the proposed model when evaluated on the testing images in the databases. In Fig. 6 to Fig. 17, the fundus images acquired from the database are referred to as 'Database image', 'Model's segmentations' are the output of the proposed model and 'Ground truths' are the images available as ground-truth in the databases.

A. RIM-ONE DATABASE

The proposed model was tested on two versions of the RIM-ONE database; version 2 and version 3. However, RIM-ONE v2 database does not have ground-truths for optic cups. The average performance of the proposed model on RIM-ONE v2 database is shown in Table I. The proposed model's best performance achieved a dice-score of 0.99 and an IOU score of 0.97. This is shown in Fig. 6. The worst performance achieved a dice-score of 0.81 and an IOU score of 0.65. The model's worst performance on the database is shown in Fig. 7.

The performance of the proposed model on RIM-ONEv3 is shown in Table II. We compared our result with that of Sevastopolsky [45], Zilly1 [26], Maninis [20] and Al-Bander [47] using the dice-score and IoU score as our assessment. The best and worst performance of the proposed model on the database is shown in Fig.8, Fig.9, Fig.10 and Fig.11 for both optic disc and optic cup segmentation.

TABLE I
OPTIC DISC SEGMENTATION PERFORMANCE FOR RIM-ONE V2 DATABASE

	RIM-ONE V2	
	Optic Disc	
	IoU Score	Dice Score
Proposed Method	0.91	0.97

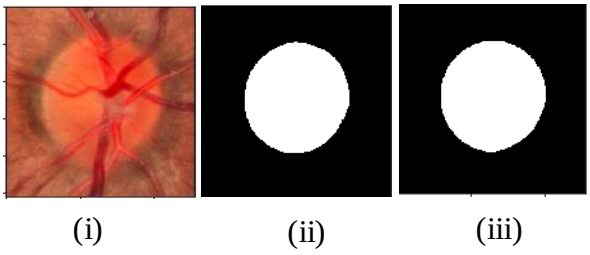

FIGURE 6. Model's best OD segmentation (i) Database image. (ii)Model's OD segmentation, (iii) Ground truth OD segmentation..

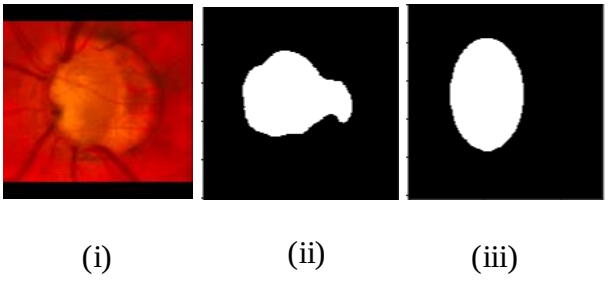

FIGURE 7. Model's worst OD segmentation (i)Database image. (ii)Model's OD segmentation, (iii) Ground truth OD segmentation.

TABLE II
OPTIC DISC AND CUP SEGMENTATION PERFORMANCE FOR RIM-ONE V3 DATABASE

	RIM-ONE v3			
	Optic Disc		Optic cup	
	IoU score	*Dice-score*	*IoU score*	*Dice-score*
Sevastopolsky [45]	0.89	0.95	0.69	0.82
Zilly1[26]	0.89	0.94	**0.80**	0.82
Maninis[20]	0.89	**0.96**	-	-
Al-Bander [47]	0.83	0.90	0.56	0.69
Proposed method	**0.90**	**0.96**	0.73	**0.86**

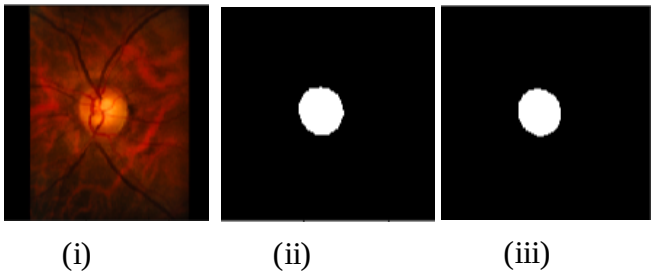

FIGURE 8. Model's best OD segmentation (i) Database image. (ii)Model's OD segmentation, (iii) Ground truth OD segmentation.

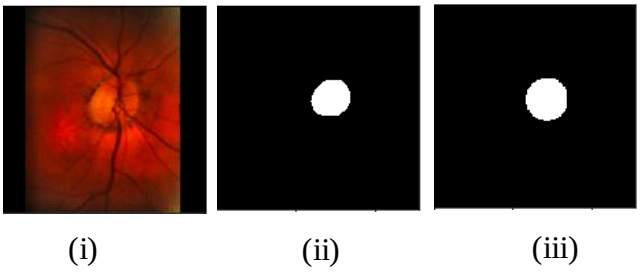

FIGURE 9. Model's worst OD segmentation (i) Database image. (ii)Model's OD segmentation, (iii) Ground truth OD segmentation.

The best optic disc segmentation as seen in Fig.8 has a dice-score of 0.99 and an IOU score of 0.96. The worst optic disc segmentation as seen in Fig.9 has a dice-score of 0.89 and an IOU score of 0.77.

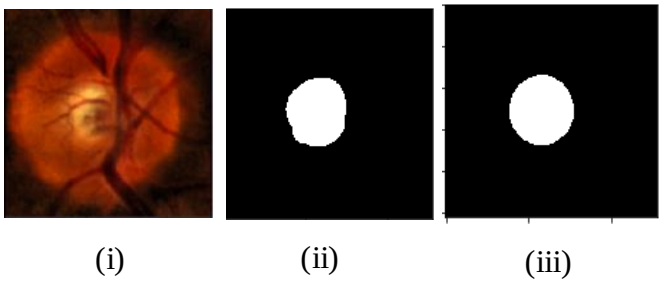

FIGURE 10. Model's best OC segmentation (i) Database image. (ii)Model's OC segmentation, (iii) Ground truth OC segmentation.

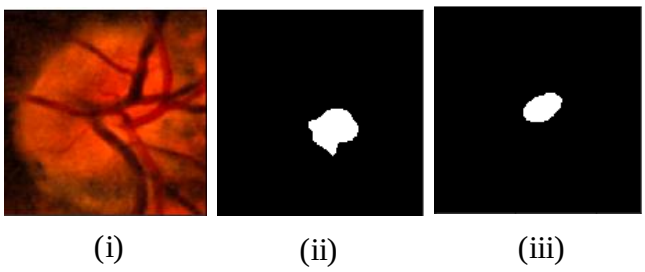

FIGURE 11. Model's worst OC segmentation (i) Database image. (ii)Model's OC segmentation, (iii) Ground truth OC segmentation.

The best optic cup segmentation as seen in Fig.10 has a dice-score of 0.98 and an IOU score of 0.91. The worst optic cup segmentation as seen in Fig.11 has a dice-score of 0.30 and an IOU score of 0.15.

B. DRISHTI-GS DATABASE

The proposed model was tested on the DRISHTI-GS database. The performance of the proposed model in this database is shown in Table III. For the optic disc segmentation, the best performance of the proposed model has a dice-score of 0.99 and an IOU score of 0.95. The best optic disc performance of the proposed model is shown in Fig. 12. The worst optic disc

performance has a dice-score of 0.95 and an IOU score of 0.84. The worst optic disc performance is shown in Fig. 13

TABLE III
OPTIC DISC AND CUP SEGMENTATION PERFORMANCE FOR DRISHTI-GS DATABASE

	DRISHTI-GS			
	Optic Disc		Optic cup	
	IoU score	*Dice-score*	*IoU score*	*Dice-score*
Sevastopolsky [45]	-	-	0.75	0.85
Zilly1[26]	**0.91**	**0.97**	0.85	0.87
Zilly2[16]	-	-	**0.86**	0.83
Al-Bander [47]	0.90	0.95	0.71	0.83
Proposed method	0.90	**0.97**	0.79	**0.95**

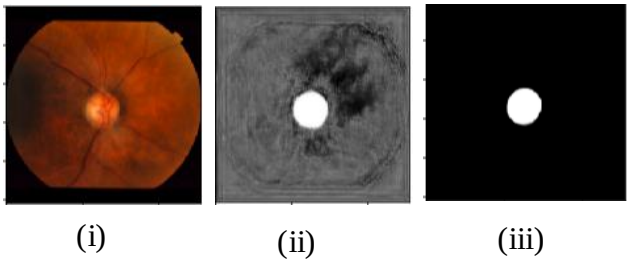

FIGURE 12. Model's best OD segmentation (i) Database image. (ii)Model's OD segmentation, (iii) Ground truth OD segmentation.

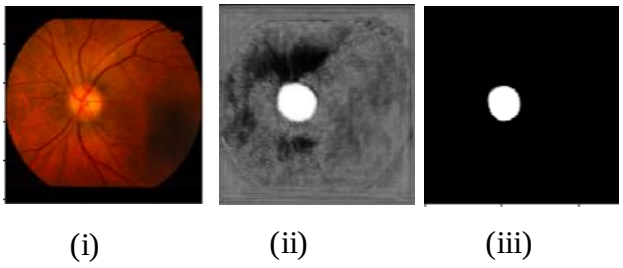

FIGURE 13. Model's worst OD segmentation (i) Database image. (ii)Model's OD segmentation, (iii) Ground truth OD segmentation.

For the optic cup segmentation, the best performance or the proposed model has a dice-score of 0.99 and an IOU score of 0.89. The best optic cup segmentation performance of the proposed model is shown in Fig. 14. The worst optic cup segmentation has a dice-score of 0.92 and an IOU score of 0.61. The worst optic cup performance is shown in Fig.15

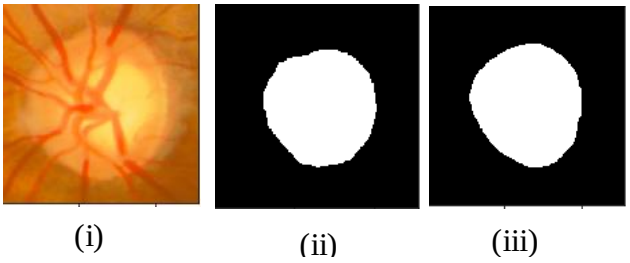

FIGURE 14. Model's best OC segmentation (i) Database image. (ii)Model's OC segmentation, (iii) Ground truth OC segmentation.

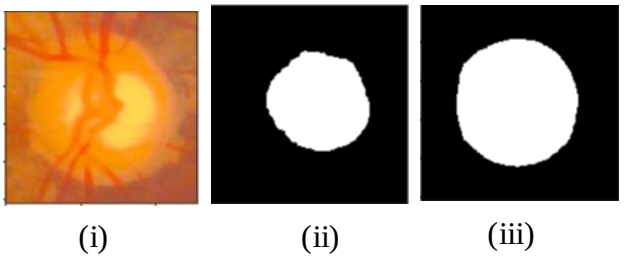

FIGURE 15. Model's worst OC segmentation (i) Database image. (ii)Model's OC segmentation, (iii) Ground truth OC segmentation.

C. DRIONS DATABASE

The model was tested on the DRIONS database. The performance of the model in this database is shown in Table IV. The DRIONS database has ground-truths only for the optic discs. The best performance of the proposed model for the optic disc segmentation has a dice sore of 0.99 and an IOU score of 0.94. The best optic disc performance of the proposed model is shown in Fig. 16. The worst optic disc segmentation performance has a dice-score of 0.95 and an IOU score of 0.82. The worst optic disc performance of the proposed model is shown in Fig. 17.

TABLE IV
OPTIC DISC SEGMENTATION PERFORMANCE FOR DRIONS DATABASE

	DRIONS	
	Optic Disc	
	IoU Score	Dice Score
Sevastopolsky [45]	0.89	0.94
Maninis [20]	0.88	**0.97**
Proposed method	**0.90**	0.96

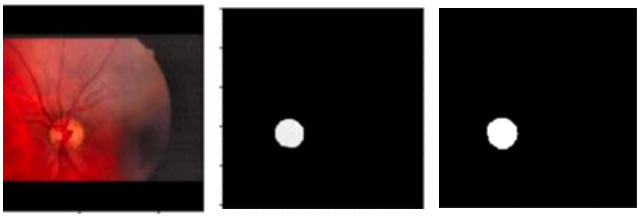

FIGURE 16. Model's best OD segmentation (i) Database image. (ii)Model's OD segmentation, (iii) Ground truth OD segmentation.

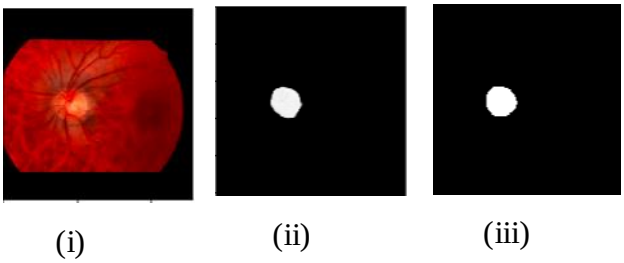

FIGURE 17. Model's worst OD segmentation (i) Database image. (ii)Model's OD segmentation, (iii) Ground truth OD segmentation.

D. XGB CLASSIFIER PERFORMANCE

The trained XGB classifier is utilized to detect glaucoma from segmented optic discs and optic cups. A popular method of detecting glaucoma from segmented optic disc and cup is the CDR (already discussed in section 1 and section 2.3). We compare the performance of CDR for glaucoma detection against that of the proposed XGB classifier. The RIM-ONE v3 and the DRISHTI-GS databases are utilized for the glaucoma detection process because they both have the optic disc and optic cup ground-truths. Furthermore, out of the four databases in view, only the RIM-ONE v3 and the DRISHTI-GS databases have each fundus image labelled appropriately as 'glaucomatous' or 'non-glaucomatous'.

Table V shows the performance in detecting glaucoma of different CDR threshold values when tested on fundus images from the RIM-ONE v3 and the DRISHTI-GS databases. The metrics utilized for comparison are Precision, Accuracy, Recall, and Area under the Receiver Operating Characteristic Curve (AUC_ROC).

TABLE V

PERFORMANCE OF DIFFERENT CDR THRESHOLD VALUES ON FUNDUS IMAGES FROM THE RIM-ONE V3 AND DRISHTI-GS DATABASES.

	CDR THRESHOLD VALUES				
	0.700	0.600	0.500	0.400	0.300
AUC_ROC	0.801	**0.874**	0.831	0.671	0.5471
ACCURACY	0.7976	**0.872**	0.832	0.6763	0.5547
RECALL	0.602	**0.795**	0.886	0.954	1.000
PRECISION	1.000	**0.945**	0.804	0.617	0.533

From Table V, it is obvious that the goodness of the CDR method for glaucoma detection is substantially influenced by the CDR threshold value in use. If a low CDR threshold value like 0.300 is utilized, the detection process will have a high recall but a very low precision i.e. although all the glaucomatous samples are recognized, numerous non-glaucomatous samples are wrongly recognized as glaucomatous. The opposite is also valid for a very high CDR threshold value. This is seen in CDR value of 0.700 (high precision, low recall). The AUC_ROC metric is a summary of the trade-off between recall and precision. Therefore, a better model will have a higher AUC_ROC value. The model proposed must have an AUC_ROC value that is higher than 0.874.

A XGB classifier was trained with all the obtained optic cup and optic disc attributes. This is done to balance off the differences caused by varying threshold values. Therefore, glaucoma can be detected from the optic cup and disc without having to decide on the threshold value to be utilized. The classifier was evaluated using 5 folds cross- validation. The performance of each cross-validation is shown in Table VI.

TABLE VI

PERFORMANCE OF THE XGB CLASSIFIER

CROSS VALIDATION SET NUMBER	AUC_ROC	ACCURACY	PRECISION	RECALL
1	0.897	0.800	0.805	0.800
2	0.961	0.896	0.897	0.897
3	0.928	0.896	0.911	0.900
4	0.947	0.896	0.899	0.895
5	0.989	0.964	0.966	0.964
6	0.852	0.821	0.836	0.821
AVERAGE VALUE	**0.929**	**0.879**	**0.886**	**0.879**

Table VI displays the result of the XGB classifier on fundus images from both the RIM-ONEv3 and DRISHTI-GS databases. The XGB classifier has an accuracy of up to 0.964 in one of the cross-validation sets. The classifier additionally accomplishes a higher AUC_ROC value than the CDR technique. It can then be concluded that the classifier has a superior classification capacity than the CDR technique.

V. DISCUSSIONS

This work developed a technique for detecting glaucoma. The first phase of the technique includes a segmentation process. The segmentation process is done using a modified U-net model. The benefits of our model include the following: the proposed model architecture has much less number of parameters to be trained. The original U-net architecture has about $3.1x10^7$ parameters while the modified architecture has about $7.8x10^5$ which is about 40x less the size of the original. The modified architecture therefore has fewer parameters to be trained. This translates to a lighter model which can be trained much faster. The proposed model also requires less training epochs. For instance, the original U-net model requires about ten (10) hours to train on a Nividia Titan GPU [37], while Sevastopolsky [45] trained his model on the RIM-ONE v3 database for about 382 epochs (this is about 3 hours of training) using the platform provided by Amazon web service. Our model was trained on the same database for 65 epochs and 32.5 minutes using Kaggle's 2 CPU cores, 14 GB RAM, 1 NVIDIA Tesla K80 GPU. This results in a cheaper cost of model training.

The second phase of the proposed glaucoma detection technique includes a trained extreme gradient boosting model. This model replaces the use of the traditional CDR method for glaucoma detection from segmented optic disc and optic cup. As discussed earlier (section 1), the traditional CDR method is very subjective and the threshold value utilized depends on the author. The CDR threshold value that has been chosen by different authors ranges from 0.3 to 0.6. The proposed extreme gradient boost (XGB) model replaces the use of CDR method. We achieved a more accurate glaucoma detection results.

VI. LIMITATION OF STUDY

In as much as the model achieves state-of-the-art results in the segmentation process, it is still affected by the poor image quality. This is truer about the optic cup segmentation. In some cases, the optic cups are extremely difficult to identify (e.g. Fig.10) in the ground-truth images and this makes the model to output a very loose approximate of the optic cup location. Also, the presence of other ocular diseases such as diabetic retinopathy are not accounted for in the glaucoma detection process. Hence, optic discs and cups labelled as 'normal' might be influenced by other visual sicknesses asides glaucoma. The impact of which isn't measured in this study.

VII. CONCLUSION

In this work, we developed a glaucoma detection model that includes two stages. The first stage includes a segmentation process and the second stage includes a glaucoma detection process. The segmentation consists of a modified U-net model that achieves state-of-the-art performance across all tested databases. The model also has a few parameters making training fast and cost effective. The glaucoma detection stage achieves high accuracy without the need to choose a CDR threshold value

VIII. FUTURE WORK

The study will be done utilizing more openly accessible databases. This will help the model to train better. Furthermore, more glaucoma detection techniques such as the ISNT ratio and area covered by blood vessels will be utilized.

REFERENCES

[1] J. Moon, K. H. Park, D. M. Kim, and S. H. Kim, "Factors Affecting ISNT Rule Satisfaction in Normal and Glaucomatous Eyes," vol. 32, no. 1, pp. 38–44, Jan. 2018, doi: 10.3341/kjo.2017.0031.

[2] K. Qiu, G. Wang, X. Lu, R. Zhang, L. Sun and M. Zhang, "Application of the ISNT rules on retinal nerve fibre layer thickness and neuroretinal rim area in healthy myopic eyes," *Acta Ophthalmologica*, vol. 96, *(2)*, pp. 161-167, 2018.

[3] A. Giangiacomo, A. L. Coleman, "The epidemiology of glaucoma". In:Glaucoma. Springer Berlin Heidelberg, pp. 13–21, 2009.

[4] P. Mitchell, W. Smith, K. Attebo and P. R. Healey, "Prevalence of open-angle glaucoma in Australia. The Blue Mountains Eye Study," *Ophthalmology*, vol. 103, *(10)*, pp. 1661, 1996. Available: https://www.ncbi.nlm.nih.gov/pubmed/8874440.

[5] G. Michelson, S. Wärntges, J. Hornegger and B. Lausen, "The papilla as screening parameter for early diagnosis of glaucoma," *Deutsches Arzteblatt International*, vol. 105, *(34-35)*, pp. 583-589, 2008. Available: https://www.ncbi.nlm.nih.gov/pubmed/19471619.

[6] P. J. Foster, F. T. S. Oen, D. Machin, T. Ng, J. G. Devereux, G. J. Johnson, P. T. Khaw and S. K. L. Seah, "The Prevalence of Glaucoma in Chinese Residents of Singapore: A Cross-Sectional Population Survey of the Tanjong Pagar District," *Archives of Ophthalmology*, vol. 118, *(8)*, pp. 1105-1111, 2000. Available: http://dx.doi.org/10.1001/archopht.118.8.1105.

[7] M. Dirani, J. G. Crowston, P. S. Taylor, P. T. Moore, S. Rogers, M. L. Pezzullo, J. E. Keeffe and H. R. Taylor, "Economic impact of primary open-angle glaucoma in Australia," *Clinical & Experimental Ophthalmology*, vol. 39, *(7)*, pp. 623-632, 2011. Available: https://onlinelibrary.wiley.com/doi/abs/10.1111/j.1442-9071.2011.02530.x.

[8] A. Almazroa, S. Alodhayb, E. Osman, E. Ramadan, M. Hummadi, M. Dlaim, M. Alkatee, K. Raahemifar and V. Lakshminarayanan, "Retinal fundus images for glaucoma analysis: The RIGA dataset," in Mar 6, 2018, pp. 105790B-8

[9] J. Jonas and A. Dichtl, "Optic disc morphology in myopic primary open-angle glaucoma," *Graefe's Arch Clin Exp Ophthalmol*, vol. 235, *(10)*, pp. 627-633, 1997. Available: https://www.ncbi.nlm.nih.gov/pubmed/9349946.

[10] J. B. Jonas, G. C. Gusek and G. O. Naumann, "Optic disc, cup and neuroretinal rim size, configuration and correlations in normal eyes [published errata appear in Invest Ophthalmol Vis Sci 1991 May;32(6):1893 and 1992 Feb;32(2):474-5]," *Investigative Ophthalmology & Visual Science*, vol. 29, *(7)*, pp. 1151, 1988. Available: http://www.iovs.org/cgi/content/abstract/29/7/1151.

[11] C. Burana-Anusorn, W. Knogprawechnon, T Kondo, S. Sintuwong and K. Tungpimolrut, "Image processing technique for glaucoma detection using the cup-to-disc ratio", in Thammasat International Journal of Science and Technology, Mar 2013, vol.19, no. 1, pp. 22-34

[12] A. Poshtyar, J. Shanbehzadeh and H. Ahmadieh, "Automatic measurement of cup to disc ratio for diagnosis of glaucoma on retinal fundus images," in Dec 2013, Available: https://ieeexplore.ieee.org/document/6746900. DOI: 10.1109/BMEI.2013.6746900.R. Nicole, "Title of paper with only first word capitalized," J. Name Stand. Abbrev., in press.

[13] H. Ahmad, A. Yamin, A. Shakeel, S. O. Gillani and U. Ansari, "Detection of glaucoma using retinal fundus images," in Apr 2014, pp. 321-324.

[14] L. Shyam and G. S. Kumar, "Blood vessel segmentation in fundus images and detection of glaucoma," in Jul 2016, Available: https://ieeexplore.ieee.org/document/7823982. DOI: 10.1109/CSN.2016.7823982.

[15] R. Panda, N. B. Puhan, A. Rao, D. Padhy and G. Panda, "Recurrent neural network based retinal nerve fiber layer defect detection in early glaucoma," in Apr 2017, pp. 692-695.

[16] G. Zilly, J. M. Buhmann and D. Mahapatra, "Boosting Convolutional Filters with Entropy Sampling for Optic Cup and Disc Image Segmentation from Fundus Images," Oct 9, 2015.

[17] Ji Sang Park, Hyeon Sung Cho and Jae Il Cho, "Automated extraction of optic disc regions from fundus images for preperimetric glaucoma diagnosis," in Oct 2017, pp. 1107-1110.

[18] E. Shelhamer, J. Long and T. Darrell, "Fully Convolutional Networks for Semantic Segmentation," Tpami, vol. 39, (4), pp. 640-651, 2017. Available: https://ieeexplore.ieee.org/document/7478072. DOI: 10.1109/TPAMI.2016.2572683.

[19] K. Simonyan and A. Zisserman, "Very Deep Convolutional Networks for Large-Scale Image Recognition," 2014. Available: http://arxiv.org/abs/1409.1556

[20] K. Maninis, J. Pont-Tuset, P. Arbeláez and L. Van Gool, "Deep Retinal Image Understanding," 2016. Available: https://arxiv.org/abs/1609.01103.

[21] R. C. Gonzalez, S. L. Eddins and R. E. Woods, Digital Image Processing using MATLAB. (2. ed., 7. repr. ed.) New Delhi [u.a.]: Tata McGraw Hill Education, 2012.

[22] H. Doğan and O. Akay, "Using AdaBoost classifiers in a hierarchical framework for classifying surface images of marble slabs," Expert Systems with Applications, vol. 37, (12), pp. 8814-8821, 2010. Available: https://www.sciencedirect.com/science/article/pii/S0957417410005233. DOI: 10.1016/j.eswa.2010.06.019.

[23] J. Sivaswamy, S. R. Krishnadas, G. Datt Joshi, M. Jain and A. Ujjwaft Syed Tabish, "Drishti-GS: Retinal image dataset for optic nerve head(ONH) segmentation," in Apr 2014, pp. 53-56.

[24] J. Sivaswamy, S. R. Krishnadas, A. Chakravarty, G. Datt Joshi, A. Ujjwaft Syed Tabish , "A Comprehensive Retinal Image Dataset for the Assessment of Glaucoma from the Optic Nerve Head Analysis", JSM Biomedical Imaging Data Papers, 2(1):1004, 2015.

[25] F. Fumero, S. Alayon, J. L. Sanchez, J. Sigut and M. Gonzalez-Hernandez, "RIM-ONE: An open retinal image database for optic nerve evaluation," in Jun 2011, pp. 1-6

[26] J. M. Buhmann, J. Zilly and D. Mahapatra, "Glaucoma detection using entropy sampling and ensemble learning for automatic optic cup and disc segmentation," *Computerized Medical Imaging and Graphics*, vol. 55, pp. 28-41, 2016. Available: https://www.clinicalkey.es/playcontent/1-s2.0-S0895611116300775.

[27] S.C. Patel and M. I. Patel, "Analysis of CDR of fundus images for glaucoma detection," in Jan 1, 2018, pp. 1071.

[28] A. Murthi and M. Madheswaran, "Enhancement of optic cup to disc ratio detection in glaucoma diagnosis," in Jan 2012, pp. 1-5.

[29] J. K. Virk, M. Singh and M. Singh, "Cup-to-disk ratio (CDR) determination for glaucoma screening," in Sep 2015, pp. 504-507.

[30] N. A. Mohamed, M.A. Zulfikley, W.M. Diyana, "An automated glaucoma screening system using cup-to-disc ratio via Simple Linear Iterative Clustering superpixel approach," Biomedical Signal Processing and Control, vol. 53, pp. 101454, 2019. Available: https://www.sciencedirect.com/science/article/pii/S1746809419300035. DOI: 10.1016/j.bspc.2019.01.003.

[31] A. Mvoulana, R. Kachouri and M. Akil, "Fully automated method for glaucoma screening using robust optic nerve head detection and unsupervised segmentation based cup-to-disc ratio computation in retinal fundus images," Computerized Medical Imaging and Graphics, vol. 77, pp. 101643, 2019. Available: https://www.sciencedirect.com/science/article/pii/S0895611119300062X. DOI: 10.1016/j.compmedimag.2019.101643.

[32] A. Murthi and M. Madheswaran, "Enhancement of optic cup to disc ratio detection in glaucoma diagnosis," in Jan 2012, pp. 1-5.

[33] F. Khan, S.A. Khan, U. U. Yasin, I. U. Haq, U.Quamar, "Detection of glaucoma using retinal fundus images," in Oct 2013, pp. 1-5.

[34] M. Roslin and S. Sumathi, "Glaucoma screening by the detection of blood vessels and optic cup to disc ratio," in Apr 2016, pp. 2210-2215.

[35] M. Lotankar, K. Noronha and J. Koti, "Detection of optic disc and cup from color retinal images for automated diagnosis of glaucoma," in Dec 2015, pp. 1-6.

[36] E. J. Carmona, M. Rinc´on, J. Garc´ıa-Feijo´o, and J. M. Mart´ınez-de-la Casa, "Identification of the optic nerve head with genetic algorithms," Artificial Intelligence in Medicine, vol. 43, no. 3, pp. 243–259, 2008

[37] O. Ronneberger, P. Fischer and T. Brox, "U-Net: Convolutional Networks for Biomedical Image Segmentation," 2015. Available: https://arxiv.org/abs/1505.04597.

[38] E. Shelhamer, J. Long and T. Darrell, "Fully Convolutional Networks for Semantic Segmentation," *Tpami*, vol. 39, *(4)*, pp. 640-651, 2017. Available: https://ieeexplore.ieee.org/document/7478072. DOI: 10.1109/TPAMI.2016.2572683

[39] H. Fu, J. Cheng, Y. Xu, D. W. K. Wong, J. Liu and X. Cao, "Joint Optic Disc and Cup Segmentation Based on Multi-Label Deep Network and Polar Transformation," *Tmi*, vol. 37, *(7)*, pp. 1597-1605, 2018. Available: https://ieeexplore.ieee.org/document/8252743.

[40] V. Iglovikov and A. Shvets, "TernausNet: U-Net with VGG11 Encoder Pre-Trained on ImageNet for Image Segmentation," 2018. Available: https://arxiv.org/abs/1801.05746.

[41] Chaurasia, A., Culurciello, E., 2017. December Linknet: exploiting encoderrepresentations for efficient semantic segmentation. In: 2017 IEEE VisualCommunications and Image Processing (VCIP), IEEE, pp. 1–4.

[42] A. O. Joshua, F. V. Nelwamondo and G. Mabuza-Hocquet, "Segmentation of optic cup and disc for diagnosis of glaucoma on retinal fundus images," in Jan 2019, pp. 183-187.

[43] S. Ioffe and C. Szegedy, "Batch Normalization: Accelerating Deep Network Training by Reducing Internal Covariate Shift," 2015. Available: https://arxiv.org/abs/1502.03167

[44] A. Maas, Awni Y. Hannun and Andrew Y. Ng, "Rectifier nonlinearities improve neural network acoustic models," in Proceedings of the 30th International Conference on Machine Learning, 2013. Available: https://ai.stanford.edu/~amaas/papers/relu_hybrid_icml2013_final.pdf

[45] A. Sevastopolsky, "Optic disc and cup segmentation methods for glaucoma detection with modification of U-Net convolutional neural network," Pattern Recognit. Image Anal, vol. 27, (3), pp. 618-624, 2017. Available: https://search.proquest.com/docview/1938627054. DOI: 10.1134/S1054661817030269.

[46] A. O. Joshua, G. Mabuza-Hocquet and F. V. Nelwamondo, "Assessment of the cup-to-disc ratio method for glaucoma detection," in Jan 2020, pp. 1-5.

[47] B. Al-Bander, B. Williams, W. Al-Nuaimy, M. Al-Taee, H. Pratt and Y. Zheng, "Dense Fully Convolutional Segmentation of the Optic Disc and Cup in Colour Fundus for Glaucoma Diagnosis," *Symmetry*, vol. 10, *(4)*, pp. 87, 2018. Available: https://search.proquest.com/docview/2040897837.

IEEE Access
Multidisciplinary | Rapid Review | Open Access Journal

Afolabi Oluwatobi Joshua

Afolabi Oluwatobi Joshua has a Master's Degree in Electrical and Electronic Engineering from the University of Johannesburg, South Africa. He is currently a doctoral student at the same University. His current research focuses on using deep learning techniques to detect glaucoma from fundus images. He has published and presented his research work both locally and internationally.

Gugulethu Mabuza-Hocquet

Gugulethu Mabuza-Hocquet has a PhD in Electrical and Electronic Engineering from the University of Johannesburg, South Africa. She is currently employed as a senior biometrics researcher at the Council for Scientific and Industrial Research (CSIR). Her current research focuses on studying the science behind the human eye and the iris by using computer vision and machine learning techniques to extract features for the automated authentication of children and adults' identity, as well as the possible detection of certain diseases. Gugulethu is a supervisor for students enrolled for Masters and PhD degrees and a mentor for permanent employees within the organization. She has published and presented her research work both locally and internationally.

Fulufhelo V. Nelwamondo

Fulufhelo Nelwamondo is an electrical engineer by training, and holds a Bachelor of Science and a PhD in Electrical Engineering, in the area of Computational Intelligence, both from the University of the Witwatersrand, in South Africa. He is a registered Professional Engineer, the Executive Manager for the CSIR Cluster: Next Generation Enterprises and Institutions, and was the Executive Director for the CSIR Modelling and Digital Science Unit. He is a Senior Member of the Institute of Electronic and Electrical Engineers (IEEE), a senior member of the Association of Computing Machinery (ACM), a member of the South African Institute of Electrical Engineers, Visiting Professor of Electrical Engineering, at the Institute of Intelligent Systems, University of Johannesburg. He was a post-doctoral fellow at the Graduate School of Arts and Sciences, of Harvard University. He is the youngest South African ever to receive the Harvard-South Africa fellowship and has been awarded many national and international research accolades, from organizations such as the IEEE, South African Institute of Electrical Engineers, amongst others.

In 2017, Prof Nelwamondo was awarded the Order of Mapungubwe in Silver, highest civilian honour bestowed by the President of the Republic of South Africa. In 2016, he was recognised by the Operation Research Society of South Africa, for outstanding contributions to the science and profession of Operation Research. Prof Fulufhelo Nelwamondo has research and practical experience in software engineering, computational intelligence and optimisation in various applications. He has interests in exciting and emerging areas of software and technology applications including data science, modelling of complex systems, machine learning, optimisation and mechanism design. He has presented his work in various countries across the world. Prof Nelwamondo has successfully supervised over 20 Masters and Doctoral degrees in Electrical Engineering and Computer Science. Prof Nelwamondo has served on

a number of Boards of entities, Advisory Committees and Panels.

Babu S. Paul

Babu Sena Paul received his B.Tech and M.Tech degree in Radiophysics and Electronics from the University of Calcutta, West Bengal, India, in 1999 and 2003 respectively. He was with Philips India Ltd from 1999-2000. From 2000-2002 he served as lecturer of Electronics and Communication Engineering Dept. at SMIT, Sikkim, India. He received his Ph.D. degree from the Department of Electronics and Communication Engineering, Indian Institute of Technology Guwahati India. He has attended and published over sixty research papers in international and national conferences, symposiums and peer reviewed journals. He has successfully supervised several postgraduate students and post-doctoral research fellows. He joined the University of Johannesburg in 2010. He has served as the Head of the Department at the Department of Electrical and Electronic Engineering Technology, University of Johannesburg from April 2015 to March 2018. He is currently serving as the Director to the Institute for Intelligent Systems, University of Johannesburg. He was awarded the IETE Research Fellowship. He is a life member of IETE and a member of IEEE.

Afolabi Oluwatobi Joshua

Afolabi Oluwatobi Joshua has a Master's Degree in Electrical and Electronic Engineering from the University of Johannesburg, South Africa. He is currently a doctoral student at the same University. His current research focuses on using deep learning techniques to detect glaucoma from fundus images. He has published and presented his research work both locally and internationally.

Gugulethu Mabuza-Hocquet

Gugulethu Mabuza-Hocquet has a PhD in Electrical and Electronic Engineering from the University of Johannesburg, South Africa. She is currently employed as a senior biometrics researcher at the Council for Scientific and Industrial Research (CSIR). Her current research focuses on studying the science behind the human eye and the iris by using computer vision and machine learning techniques to extract features for the automated authentication of children and adults' identity, as well as the possible detection of certain diseases. Gugulethu is a supervisor for students enrolled for Masters and PhD degrees and a mentor for permanent employees within the organization. She has published and presented her research work both locally and internationally.

Fulufhelo Nelwamondo

Fulufhelo Nelwamondo is an electrical engineer by training, and holds a Bachelor of Science and a PhD in Electrical Engineering, in the area of Computational Intelligence, both from the University of the Witwatersrand, in South Africa. He is a registered Professional Engineer, the Executive Manager for the CSIR Cluster: Next Generation Enterprises and Institutions, and was the Executive Director for the CSIR Modelling and Digital Science Unit. He is a Senior Member of the Institute of Electronic and Electrical Engineers (IEEE), a senior member of the Association of Computing Machinery (ACM), a member of the South African Institute of Electrical Engineers, Visiting Professor of Electrical Engineering, at the Institute of Intelligent Systems, University of Johannesburg. He was a post-doctoral fellow at the Graduate School of Arts and Sciences, of Harvard University. He is the youngest South African ever to receive the Harvard-South Africa fellowship and has been awarded many national and international research accolades, from organizations such as the IEEE, South African Institute of Electrical Engineers, amongst others.

In 2017, Prof Nelwamondo was awarded the Order of Mapungubwe in Silver, highest civilian honour bestowed by the President of the Republic of South Africa. In 2016, he was recognised by the Operation Research Society of South Africa, for outstanding contributions to the science and profession of Operation Research. Prof Fulufhelo Nelwamondo has research and practical experience in software engineering, computational intelligence and optimisation in various applications. He has interests in exciting and emerging areas of software and technology applications including data science, modelling of complex systems, machine learning, optimisation and mechanism design. He has presented his work in various countries across the world. Prof Nelwamondo has successfully supervised over 20 Masters and Doctoral degrees in Electrical Engineering and Computer Science. Prof Nelwamondo has served on

a number of Boards of entities, Advisory Committees and Panels.

Babu S. Paul

Babu Sena Paul received his B.Tech and M.Tech degree in Radiophysics and Electronics from the University of Calcutta, West Bengal, India, in 1999 and 2003 respectively. He was with Philips India Ltd from 1999-2000. From 2000-2002 he served as lecturer of Electronics and Communication Engineering Dept. at SMIT, Sikkim, India. He received his Ph.D. degree from the Department of Electronics and Communication Engineering, Indian Institute of Technology Guwahati India. He has attended and published over sixty research papers in international and national conferences, symposiums and peer reviewed journals. He has successfully supervised several postgraduate students and post-doctoral research fellows. He joined the University of Johannesburg in 2010. He has served as the Head of the Department at the Department of Electrical and Electronic Engineering Technology, University of Johannesburg from April 2015 to March 2018. He is currently serving as the Director to the Institute for Intelligent Systems, University of Johannesburg. He was awarded the IETE Research Fellowship. He is a life member of IETE and a member of IEEE.